University of Szeged

Faculty of Pharmacy

Institute of Pharmaceutical Technology and Regulatory Affairs

Head: Prof. Dr. Ildikó Csóka, Pharm.D., Ph.D.

Summary of Ph.D. Thesis

IMPROVING THE ABSORPTION OF POORLY PERMEABLE DRUGS THROUGH ALTERNATIVE DELIVERY ROUTES USING NANOCARRIERS

By

Maryana Yahia Salamah, Pharm.D., M.Sc.

pharmacist

Supervisors:

Prof. Dr. György Tibor Balogh D.Sc.

Dr. habil. Gábor Katona, Ph.D.

Szeged

2025

University of Szeged

Doctoral School of Pharmaceutical Sciences

Head: Prof. Dr. Judit Hohmann, D.Sc

Educational Program: Pharmaceutical Technology

Head: Prof. Dr. Ildikó Csóka, Ph.D.

Institute of Pharmaceutical Technology and Regulatory Affairs

Supervisors: Prof. Dr. György Tibor Balogh D.Sc., Dr. habil. Gábor Katona, Ph.D.

Maryana Yahia Salamah

IMPROVING THE ABSORPTION OF POORLY PERMEABLE DRUGS THROUGH ALTERNATIVE DELIVERY ROUTES USING NANOCARRIERS

Complex Exam Committee:

Head: **Prof. Dr. Piroska Szabó-Révész**, D.Sc., Institute of Pharmaceutical Technology and Regulatory Affairs, University of Szeged.

Members: **Dr. Gabriella Csóka, Ph.D.,** Meditop Pharmaceutical Ltd. Pilisborosjenő.

Dr. Tamás Sovány, Ph.D., Institute of Pharmaceutical Technology and Regulatory Affairs, University of Szeged.

Reviewer Committee:

Head: **Prof. Dr. Zsolt Szakonyi, DSc**, University of Szeged, Faculty of Pharmacy, Institute of Pharmaceutical Chemistry.

Reviewers: **Dr. László Janovák, PhD,** University of Szeged, Faculty of Science and Informatics, Department of Physical Chemistry and Materials Science.

Dr. Szilvia Veszelka, PhD, HUN-REN Biological Research Center Szeged, Institute of Biophysics, Molecular Neurobiology Group.

Members: **Dr. Péter Doró, PhD,** University of Szeged, Faculty of Pharmacy, Department of Clinical Pharmacy.

Dr. Dóra Rédei, PhD, University of Szeged, Faculty of Pharmacy, Institute of Pharmacognosy.

Szeged

2025

Abbreviations

Abbreviation	Description	Abbreviation	Description
ANOVA	Analysis of variance	**HLB**	Hydrophilic-lipophilic balance
AP	Ascorbyl palmitate	**HSA**	Human serum albumin
ASPs	Aspasomes	**IN**	Intranasal
AUC	Area under the curve	**IVIVC**	In vitro-in vivo correlations
BBB	Blood-brain-barrier	**k_e**	Elimination rate constant
BCS	Biopharmaceutics classification system	**LAM**	Lamotrigine
BCSFB	Blood-cerebrospinal fluid barrier	**LAM-BSA**	Lamotrigine-loaded bovine serum albumin nanoparticles
BSA	Bovine serum albumin	**LOD**	Limit of detection
Caco-2	Human colon adenocarcinoma	**LOQ**	Limit of quantification
CH	Cholesterol	**MDT**	Mean dissolution time
Cmax	Maximum concentration	**MeOH**	Methanol
CNS	Central nervous system	**MRT**	Mean residence time
CSF	Cerebrospinal fluid	**NPs**	Nanoparticles
DL	Drug loading	**PDI**	Polydispersity index
DoE	Design of Experiments	**PK**	Pharmacokinetic
DPBS	Dulbecco's phosphate-buffered saline	**PNS**	Peripheral nervous system
EE	Encapsulation efficiency	**R^2**	Correlation coefficient
EtOH	Ethanol	**RED**	Rapid equilibrium dialysis
F%	Relative bioavailability	**SD**	Standard deviation
FAV	Favipiravir	**SNES**	Simulated nasal electrolyte solution
FAV-ASP	Favipiravir-loaded aspasomes	**$t_{1/2}$**	Elimination half-life
GC-MS	Gas chromatograph-mass spectrometric	**ZP**	Zeta potential

1. INTRODUCTION

The increasing prevalence and severity of central nervous system (CNS) disorders pose a serious, life-threatening condition, which could cause lifelong disability or could be associated with sudden death. CNS disorders include acute brain injury and cerebrovascular diseases (such as stroke, cerebral ischemia, and epilepsy), and neurodegenerative diseases (such as Alzheimer's, Parkinson's, and Huntington’s diseases).

The drug discovery for CNS disorders is a long-term, expensive process with a low success rate in clinical trials, which is associated with the physiological barriers that impede drug permeation, including the blood-brain-barrier (BBB) and blood-cerebrospinal fluid barrier (BCSFB). Therefore, the pharmaceutical research has been focused on improving the BBB permeability of the marketed drugs by developing suitable drug carriers and using alternative routes of administration.

Epilepsy, the second common CNS disorder caused by abnormal electrical activity in the brain, and is characterized by recurrent unprovoked epileptic seizures. Seizures are also a primary symptom of viral infections of the CNS, which could occur during the infection or after recovery and result in acquired epilepsy. Several viruses, especially neurotropic RNA viruses, are contributing in the development of seizures and epilepsy by the disrupting in the integrity of BBB and BCSFB following invasion of the brain through the nasal epithelium, or the choroid plexus into the CSF, or the pseudounipolar sensory neurons of the peripheral nervous system (PNS).

In recent decades, intranasal (IN) administration has emerged in pharmaceutical research as a promising non-invasive strategy for targeted drug delivery to the brain, via the olfactory nerve pathway, olfactory mucosal epithelial pathway, trigeminal nerve pathway, and blood circulation pathway.

IN administration requires selecting an appropriate drug delivery system to overcome the physiological barriers in both nasal cavity (such as mucus barrier, mechanism of mucociliary clearance, enzymatic activity and tight junctions in the olfactory epithelium), and the brain (such as tight junctions in BBB, pericytes and astrocytes, efflux transporters and metabolic enzymes) which limit the permeation of ~ 98% of the drugs. Therefore, the physicochemical properties of the drug delivery system, including lipophilicity, biodegradability, particle size, surface charge, and mucoadhesion properties, have a crucial role in facilitating effective drug absorption and distribution of the drug from the nasal cavity to the brain. Accordingly,

nanoparticles provide a promising drug delivery for CNS targeting and overcome the limits of conventional pharmaceutical formulations.

Nanoparticles (NPs) have been used in many studies for nose-to-brain delivery system due to their advantages, including promoting drug accumulation in the CNS through an increased permeation across the olfactory region, protecting the drug from enzymatic degradation, and prolonging nasal residence time.

Several types of nanoparticles, including lipid-based formulations such as liposomes, niosomes, and aspasomes, as well as albumin-based nanoparticles like bovine serum albumin (BSA) nanoparticles, have been developed to enhance the delivery of drugs to the CNS, depending on their surface area, surface charge, solubility, viscosity and biodegradability.

In this research, we selected aspasomes, as a lipid nanocarrier, and bovine serum albumin nanoparticles as drug carriers for antiviral drug (Favipiravir; FAV) and antiepileptic drug (Lamotrigine; LAM), respectively.

2. AIM OF THE WORK

- This Ph.D. work aimed to develop and characterize two novel nanocarrier systems for possible nose-to-brain delivery of lamotrigine and favipiravir (lamotrigine-loaded bovine serum albumin nanoparticles and favipiravir-loaded aspasomes) as poorly permeable model CNS active drugs intended for the treatment of epilepsy and neurotropic RNA virus infections.
- This Ph.D. work was designed and studied according to the following steps:

- Performing a systematic literary review about epilepsy and CNS viral infection, as well as lipid and albumin nanoparticles as suitable nano-drug delivery systems for nose-to-brain delivery .
- Determining the factors which could influence the preparation of lamotrigine-loaded bovine serum albumin nanoparticles, and use full factorial design for the optimization.
- Determining the factors which could influence the preparation of favipiravir-loaded aspasomes.
- Performing *in vitro* evaluation of both optimized nanocarriers, regarding to physical and chemical properties, and nasal applicability.
- Conducting *in vitro* cell line studies to evaluate the cytotoxicity of lamotrigine-loaded bovine serum albumin nanoparticles.
- Carrying out *ex vivo* studies using human nasal mucosa to predict the permeability through the nasal epithelium for both optimized nanocarriers.
- Performing *in vivo* studies to evaluate the bioavailability of favipiravir-loaded aspasomes in plasma and CSF samples.

3. MATERIALS

LAM (6-(2,3-dichlorophenyl)-1,2,4-triazine-3,5-diaminutese), was purchased from Teva Ltd. (Budapest, Hungary). BSA cell culture grade, ethanol (EtOH) (96% v/v), methanol (MeOH) 99.99 % v/v (HPLC grade), dimethyl sulfoxide (DMSO), mannitol, sodium chloride for physiological salt solution, and anhydrous disodium hydrogen phosphate were purchased from Molar Chemicals Ltd. (Budapest, Hungary). Dodecane and hexane were purchased from Merck KGaA (Darmstadt, Germany). Polar brain lipid extract, porcine stomach mucin (Type III), 1-(3-dimethylaminutesopropyl)-3-ethylcarbodiimide hydrochloride (EDC) were purchased from Sigma Aldrich Co. Ltd. (Budapest, Hungary). Dulbecco's phosphate-buffered saline (DPBS) was acquired from Capricorn Scientific GmbH (Ebsdorfergrund, Germany). As nasal dissolution medium, Simulated Nasal Electrolyte Solution (SNES) was freshly prepared, which consisted of 8.77 g sodium chloride (NaCl), 2.98 g potassium chloride (KCl), 0.59 g and anhydrous calcium chloride (CaCl2) dissolved in 1000 mL of deionized water at pH 5.6. These chemicals were acquired from Sigma-Aldrich Co., Ltd. (Budapest, Hungary).

FAV was provided by Egis Pharmaceuticals Plc. (Budapest, Hungary) with a purity of 99.6% w/w (according to the supplier certificate of analysis). Anhydrous disodium hydrogen phosphate were purchased from Molar Chemicals Kft. (Budapest, Hungary). Acetonitrile 99.8% v/v (HPLC grade) was purchased from PromoChem (Wesel, Germany). Ascorbyl acid-6-palmitate (AP), sorbitan monostearate (Span® 60) and chloroform were purchased from Merck KGaA (Darmstadt, Germany). In all experiments, purified water was filtered using the Millipore Milli-Q® (Merck Ltd., Budapest, Hungary) Gradient Water Purification System.

4. METHODS

4.1. Preparation and optimization of lamotrigine-loaded bovine serum albumin nanoparticles (LAM-BSA)

The coacervation method was used to prepare lamotrigine-loaded bovine serum albumin nanoparticles (LAM-BSA). Firstly, BSA was dissolved in 3 mL of 5 mM NaCl solution under magnetic stirring for 15 min at 40 ˚C. Then, LAM was added to the BSA solution, and the pH was adjusted to 8 with 0.1 N NaOH. Secondly, 15 mL of EtOH was injected dropwise with a flow rate of 1 mL/min until turbidity appeared in the solution. The amount of BSA, the amount of LAM and stirring speed were selected for formulation optimization using Design of Experiments (DoE).

A 3^3 factorial design was used to evaluate the relationship between independent variables (amount of BSA, amount of LAM and stirring speed) and their responses on average

hydrodynamic diameter (Y1: Z-average) and encapsulation efficiency (Y2: EE%), as shown in Table 2. The TIBCO Statistica® 13.4 software (Statsoft Hungary, Budapest, Hungary) was used for DoE, quadratic response surface analysis of 2D and 3D plots, and to construct a second-order polynomial model. The relationship of the variables on the response can be analysed by the following second-order equation (1):

$$Y = \beta_0 + \beta_1 X_1 + \beta_2 X_2 + \beta_3 X_3 + \beta_{11} X_1^2 + \beta_{22} X_2^2 + \beta_{33} X_3^2 + \beta_{12} X_1 X_2 + \beta_{13} X_1 X_3 + \beta_{23} X_2 X_3 \quad (1)$$

Where Y is the response variable; β_0 is a constant; β_1, β_2, and β_3 are linear coefficients; β_{12}, β_{13}, and β_{23} are interaction coefficients between the three factors; and β_{11}, β_{22}, and β_{33} are quadratic coefficients.

Table 1. Independent variables of the 3^3 factorial design

Independent variables	Levels		
	Low (-1)	Medium (0)	High (+1)
X1: Amount of BSA (mg)	10	20	30
X2: Amount of LAM (mg)	10	20	30
X3: Stirring speed (rpm)	500	750	1000

After selecting the optimal formulation, 1 mg of EDC was added during the preparation process as a cross-linking agent for the stabilization of the nanoparticles after adding EtOH. The cross-linking reaction was conducted for 2 h incubation time at 40˚C using a magnetic stirrer. Then, EtOH was evaporated at 40 ˚C for 30 min under pressure using vacuum drying chambers (Binder GmbH, Tuttlingen, Germany), and the pellets were redispersed in purified water using an ultrasonication bath. The resulting suspension was purified using a Hermle Z323 laboratory centrifuge (Hermle AG, Gossheim, Germany) at 14000 rpm for 15 min at 4 ± 1˚C. Finally, the pellets were redispersed in purified water to the original volume by using an ultrasonication bath.

4.2. Preparation of favipiravir-loaded aspasomes (FAV-ASP)

Nonionic surfactant-based favipiravir-loaded aspasomes (FAV-ASP) were prepared using a film hydration method. Firstly, the lipid solution was prepared by dissolving AP, Span® 60 and CH in 10 mL of chloroform. Secondly, a fixed amount of FAV (30 mg) was dissolved in 5 mL of MeOH (Table 2). Then, FAV solution was mixed with the lipid solution in a round bottom flask, and the organic solvent was evaporated at 60 ℃ and 633 mbar pressure using a Büchi R-210 rotary vacuum evaporator (Flawil, Switzerland), and the rotation was set at 100 rpm for 1 h, until the appearance of a thin film on the wall of the flask. Finally, the thin lipid film was hydrated with 15 mL of pH 7.4 phosphate-buffered saline (PBS) for 1 h.

Table 2. The composition of FAV-ASP formulations

Formulation	Nonionic Surfactant-Based FAV-ASP			
	FAV (mg)	AP (mg)	Span ® 60 (mg)	CH (mg)
FAV-ASP1	30	25	25	50
FAV-ASP2	30	25	50	50
FAV-ASP3	30	50	25	50
FAV-ASP4	30	50	50	50

4.3. Combined methods for LAM-BSA and FAV-ASP formulations

4.3.1. Freeze-drying

Freeze-drying was conducted with a Scanvac, CoolSafe 100-9 Pro type apparatus (LaboGeneApS, Lynge, Denmark). 1.5 mL of all formulations was lyophilized in the presence of 5% w/v mannitol as a cryoprotectant. Freeze-drying was carried out at – 40 ˚C for 16 h under a pressure of 0.012 mbar with an additional 4 h of secondary drying at 25 ˚C. The process was controlled by the Scanlaf CTS16a02 software. The samples were then stored in the refrigerator until further investigation

4.3.2. Vesicle size analysis, polydispersity index and zeta potential determination

The average hydrodynamic diameter (Z-average), polydispersity index (PDI), and zeta potential (ZP) values of the prepared formulations were evaluated by measuring the dynamic light scattering using a Zetasizer apparatus (Malvern Instrument Ltd., Worcestershire, UK). The measurements were performed in triplicate. The results were presented as means ± SD.

4.3.3. Drug content

Drug content of both LAM-BSA and FAV-ASP formulation was determined as follows: the formulations were redispersed in distilled water, and then 1 mL of the formulations was diluted with 4 mL of methanol using ultrasonication bath for 10 min. After that, the suspensions were filtered using 0.45 µm syringe filters, and LAM concentration was determined using an Agilent 1260 HPLC (Agilent Technologies, San Diego, CA, USA) equipped with a Kinetex® C18 column (5 µm, 150 mm * 4.6 mm, 100 A°). The mobile phase consisted of Methanol: Phosphate buffer (pH 3.5, 10 mM) in a 30:70 (v/v) ratio. The injection volume was 10 µL, with a flow rate of 1 mL/min at 30˚C. Chromatograms were detected at 275 nm. The regression coefficient of the calibration was 0.9997, while the limit of quantification (LOQ) and the limit of detection (LOD) of LAM were 0.016 and 0.049 ppm, respectively. Data were evaluated using ChemStation B.04.03. Software (Agilent Technologies, Santa Clara, USA).

On the other hand, FAV concentration was determined using the same instrument equipped with a Zorbax® SB-CN C18 column (5 μm, 250 mm × 4.6 mm, 100 Å). The mobile phase was acetonitrile–disodium hydrogen phosphate anhydrous buffer (pH 3.1, 20 mM) in a 10:90 (v/v) ratio. The injection volume was 10 μL, with a flow rate of 1 mL/min at 30˚C. Chromatograms were detected at 323 nm. The regression coefficient of the calibration was 0.9996, while LOQ and LOD of FAV were 0.039 and 0.009 ppm, respectively. Data were evaluated using the same software.

4.3.4. Encapsulation efficiency

The encapsulation efficiency (EE%) is defined by the percentage of the drug that is successfully entrapped into the nanoparticles. The EE% of LAM was determined using centrifugation method. Additionally, the EE% of FAV was determined using the dialysis method.

4.3.5. In vitro drug release study under nasal conditions

The drug release test under nasal conditions was conducted using the paddle method (Hanson SR8 Plus (Teledyne Hanson Research, Chatsworth, CA, USA)). The freeze-dried samples were redispersed in SNES (pH 5.6, with a theoretical concentration of 2 mg/mL for both LAM and FAV). Pretreated dialysis membranes (Spectra / Por®,Spectrum Laboratories Inc., Rancho Dominguez, CA, USA) with a molecular weight cut-off value (MWCO) of 12-14 kDa were loaded with 1 mL of the reference suspensions and the samples. The bags were sealed at both ends. 100 mL of SNES was used as a dissolution medium. The measurement was carried out at 32˚C at a paddle rotation speed of 50 rpm, while sampling was carried out for 30 min. Quantification of aliquots was performed by HPLC. Three parallel measurements were performed, and data were presented as means ± SD.

4.3.6. Ex vivo nasal permeability study on human nasal mucosa

The *ex vivo* transmucosal permeability of the optimized formulations (LAM-BSA and FAV-ASP) and reference suspensions of LAM and FAV (with 2 mg/mL nominal concentration) was studied in a modified Side-Bi-Side® type horizontal diffusion apparatus under artificial nasal conditions. The experiments have been performed under the approval of the University of Szeged's institutional ethics committee (ETT-TUKEB: IV/3880-1/2021/EKU). Nasal mucosa was cut with a surgical scalpel into uniform segments with a

diameter of 6 mm, and inserted between donor and acceptor phases to provide an appropriate surface for permeability study. To the donor phase 8 mL of SNES was added, whereas to the acceptor phase, 9 mL of DPBS solution (pH 7.4) was pipetted. For the measurement, both reference suspensions and selected freeze-dried formulations were redispersed in 1 mL SNES, and added to the donor compartment. Both compartments were continuously stirred at 300 rpm using magnetic stirrers. Aliquots were withdrawn (100 μL) from the acceptor phase at 5, 10, 15, 30, and 60 min and replaced with fresh DPBS. The concentrations were determined using HPLC.

4.4. Methods related to characterization of LAM-BSA

4.4.1. Cytotoxicity assay

Cytotoxicity was determined by the MTT assay on the human colon adenocarcinoma (Caco-2) cell line at six different concentrations (5, 10, 25, 50, 100, and 250 μM for LAM). Caco-2 cells were kindly donated by Solvo Biotechnology (Szeged, Hungary). Cell viability was assessed using the statistical software GraphPad Prism 10.12

4.5. Methods related to characterization of FAV-ASP

4.5.1. In vivo study

Healthy male Sprague-Dawley rats (339 ± 39 g, mean ± SD) were anaesthetized with an *i.p.* injection of ketamine (50 mg/kg) and xylazine (10 mg/kg). The femoral vein was cannulated for plasma collection. A total of 50 μL FAV (2 μg/μL) or the corresponding formulation of FAV was administered nasally. Animals were divided into two groups (FAV and optimal FAV-ASP), and 0.5 mL of blood samples were taken at 0, 5, 10, 15, 30 and 60 min post-FAV administration, then CSF samples were collected at the end of the experiments. After 45 min, the clot was removed by centrifuging at 1000 x g for 10 min. The resulting supernatant (non-hemolytic serum) was extracted with 2 volumes of acetonitrile. The precipitate was removed by centrifuging at 1000 × g for 10 min. FAV was measured by GC-MS using a Shimadzu GCMS-QP2010 (Shimadzu, Kyoto, Japan) equipment.

4.5.2. Evaluation of pharmacokinetic (PK) parameters

The PK parameters of initial FAV and FAV-ASP1 were determined in the plasma and the CSF following a single intranasal dose to evaluate the brain targeting. PK Solver 2.0 software was used to determine PK parameters by non-compartmental analysis.

5. Statistical analysis

All results are expressed as mean ± SD. GraphPad Prism version 10.12 software (GraphPad Software, San Diego, CA) was used for the statistical analysis. A one-way analysis of variance (ANOVA) and Tukey's post-hoc test were performed to compare the groups. A significant level was set at a p value < 0.5. Where (ns) means non-significant, *p-value < 0.05, **p-value < 0.01, and ***p-value < 0.001, ****p-value <0.0001.

6. RESULTS AND DISCUSSION

6.1. Results of LAM-BSA characterization

6.1.1. Preparation and optimization of LAM-BSA

LAM-BSA nanoparticles were prepared using the coacervation method, which is one of the most commonly used processes to prepare albumin nanoparticles. In this study, we studied the effect of BSA amount (X1), LAM amount (X2) and the stirring speed (X3) on the Z-average (Y1) and EE% (Y2) of the prepared nanoparticles at 3 levels (Table 3).

Table 3. Dependent and independent factors of the 3^3 factorial design. Results are presented as mean ± SD

Formulation Code	Independent factors			Responses	
	BSA (mg)	LAM (mg)	Stirring speed (rpm)	Z-average (nm)	EE (%)
LAM-NP-1	10	10	500	184.90 ± 0.82	62.76 ± 4.53
LAM-NP-2	10	20	1000	212.50 ± 1.73	83.01 ± 4.29
LAM-NP-3	10	30	750	218.83 ± 3.00	89.290 ± 2.88
LAM-NP-4	20	10	1000	205.77 ± 2.51	66.56 ± 3.94
LAM-NP-5	20	20	750	223.23 ± 2.24	83.27 ± 5.60
LAM-NP-6	20	30	500	182.73 ± 1.58	89.59 ± 3.45
LAM-NP-7	30	10	750	195.87 ± 0.85	64.84 ± 2.09
LAM-NP-8	30	20	500	168.90 ± 4.04	86.53 ± 3.11
LAM-NP-9	30	30	1000	173.80 ± 1.25	± 2.46 91.78

A. The impact of independent factors on Z-average (Y1)

A quadratic equation describing the individual main effects of X_1, X_2, and X_3 on Y_1 was generated by the reduced linear mathematical model, as presented in equation (2):

$$Y1 = 196.281 - 12.944X_1 - 1.861X_2 + 9.255X_3 + 3.994X_1^2 + 3.947X_2^2 + 12.272X_3^2 - 3.455X_1X_2 \quad (2)$$

The regression coefficient (R^2) of the surface plot was 0.999, the adjusted R^2 was 0.997 and the MS Residual was 0.022, indicating a proper correlation. Analysis of variance (ANOVA) was applied as statistics, with a 95% confidence interval level, where the variable was considered significant if the p-value < 0.05. The model factors such as X_1, X_3, X_1^2 were significant (p-value < 0.05). Furthermore, the positive value of the coefficient implies that Z-average increases with the factor, and the negative value implies that Z-average increases with decreasing the factor (Figure 1).

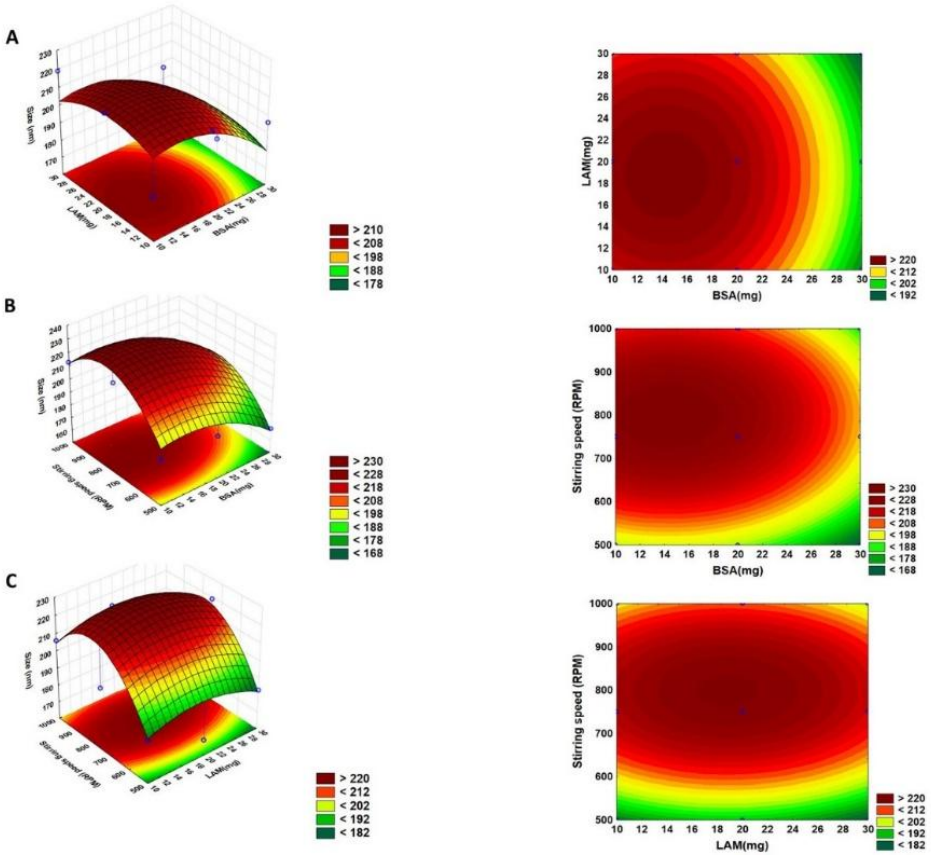

Figure 1. Contour plots (2D) and response surface plots (3D) of selected independent factors on Z-average; (A): BSA amount (X_1) and LAM amount (X_2), (B): BSA amount (X_1) and stirring speed (X_3), (C): LAM amount (X_2) and stirring speed (X_3).

B. The effect of independent factors on EE%

A quadratic equation describing the individual main effects of X_1, X_2, and X_3 on Y_2 was generated by the reduced linear mathematical model, as presented in equation (3):

$$Y2 = 79.737 + 1.348X_1 + 12.747X_2 + 3.4X_2^2 \quad (3)$$

The regression coefficient (R^2) of the surface plot was 0.992, the adjusted R^2 was 0.988, and the MS Residual was 1.545, which indicates a proper correlation. The model factors such as X_1, X_2, X_2^2 were significant (p-value < 0.05, p-value < 0.001, p-value < 0.001, respectively), and had positive effects. The results showed that the EE% increased with increasing amount of BSA (Figure 2).

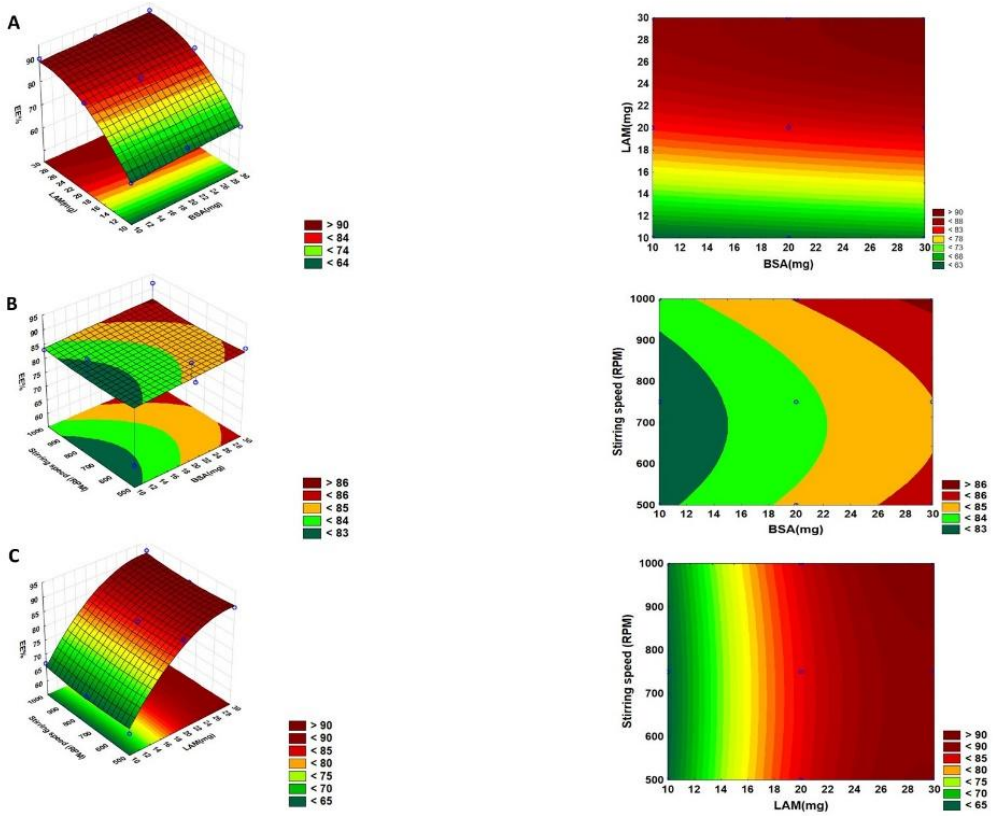

Figure 2. Contour plots (2D) and response surface plots (3D) of selected independent factors on EE%; (A): BSA amount (X_1) and LAM amount (X_2), (B): BSA amount (X_1) and stirring speed (X_3), (C): LAM amount (X_2) and stirring speed (X_3).

Based on these results, the selected LAM-NP was prepared using: BSA (30 mg), LAM (30 mg), and the stirring speed (1000 rpm). The particle size was 173.80 ± 1.25 nm with a narrow particle size distribution (PDI = 0.21 ± 0.01), a negative ZP value (-29.80 ± 0.07 mV) and a high EE% value (91.78 ± 2.46 %). This formulation was used for the cross-linking reaction with EDC (1 mg) to prepare the optimal LAM-BSA formulation. The freeze-dried LAM-BSA formulation (with Z-average of 163.77 ± 1.96 nm, PDI of 0.16 ± 0.01, ZP value of -33.97 ± 0.59 mV, and a high EE% value of 97.31 ± 0.17 %) was used for further investigations.

6.1.2. In vitro drug release at nasal conditions

LAM is a BCS Class II drug, and its dissolution is the rate-limiting step for its absorption. Since LAM is a weak base, it may not have dissociated efficiently above its pKa value (5.7), which limits drug solubilization at pH 5.6, which could be responsible for the lower degree of drug release from BSA nanoparticles. The results demonstrated that there was no significant difference in the release profile of LAM-BSA formulation and initial LAM up to 30 min (Figure 3).

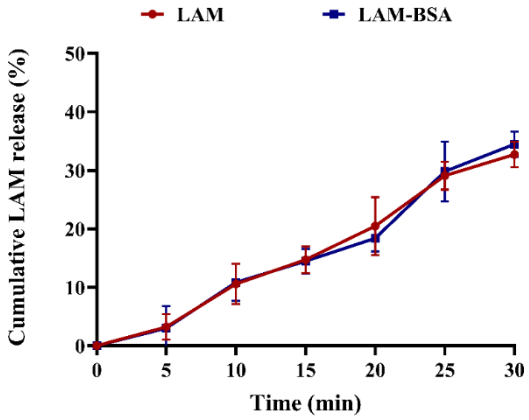

Figure 3. Cumulative *in vitro* release profile of LAM-BSA in comparison with the initial LAM. Results are expressed as means ± SD (n = 3).

6.1.3. Ex Vivo Nasal Permeability Study on Human Nasal Mucosa

Human nasal mucosa has been used to predict the absorption of the LAM-BSA formulation through the nasal cavity, and to predict the penetration across the BBB. The result demonstrated that the optimal formulation exhibited a significantly higher cumulative permeated amount of LAM compared to the initial LAM (p-value < 0.05), (260.61 ± 0.66 and 841.71 ± 2.09 µg/cm^2 for LAM and LAM-BSA, respectively), as shown in Figure 4.

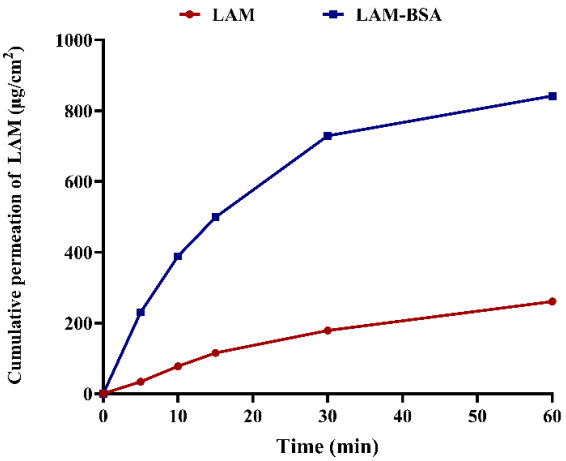

Figure 4. Ex vivo permeability study of the optimal formulations in comparison with initial LAM on human nasal mucosa. Results are expressed as means ± SD (n = 3).

6.1.4. Cytotoxicity assay

The percentage of cell viability was determined after incubation the cells with LAM at a concentration of 5-250 µM for 2 h. The results were presented in Figure 5. This result indicated that LAM-BSA formulation is non-toxic (cell viability > 70 %), and the use of BSA nanoparticles could be a suitable and compatible drug carrier for LAM.

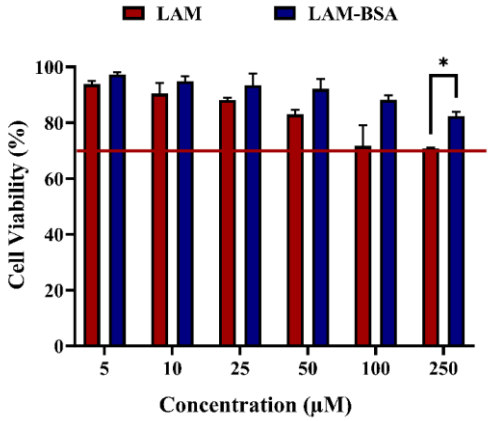

Figure 5. Cell viability % of LAM-BSA formulation in comparison to the initial LAM. Results are expressed as means ± SD (n = 3). *p-value < 0.05.

6.2. Results of FAV-ASP characterization

6.2.1. Preparation and optimization of FAV-ASP

FAV-ASP formulations were prepared by combining different amounts of AP and nonionic surfactants (Span® 60) with fixed amount of CH. For the optimization, we first selected formulations based on the acceptable parameters of the drug carrier for the nose-to-brain delivery system, which include: a Z-average of 150–300 nm, PDI < 0.5, ZP > |±30| mV, EE% > 50%, and DL% > 10%, to be evaluated using BBB-PAMPA.

As presented in Table 4, only FAV-ASP4 had a Z-average > 300 nm; therefore, we excluded it from the evaluation. On the other hand, FAV-ASP2 showed EE% and DL% values out of the acceptable range; thus, we also excluded it from further investigation.

Table 4. Z-average, PDI, ZP and EE% values of the prepared formulations. Results are expressed as means ± SD (n = 3).

Formulation	Z-average (nm)	PDI	ZP (mV)	EE (%)	DL%
FAV-ASP1	292.06 ± 2.10	0.36 ± 0.03	-74.73 ± 3.28	55.33 ± 0.41	12.79 ± 0.22
FAV-ASP2	292.76 ± 3.80	0.31 ± 0.05	-73.16 ± 4.65	48.35 ± 0.38	9.374± 0.07
FAV-ASP3	284.60 ± 6.70	0.29 ± 0.06	-65.66 ± 2.70	53.48 ± 0.26	10.36 ± 0.41
FAV-ASP4	341.20 ± 8.88	0.40 ± 0.04	-72.82 ± 1.20	-	-

The formulations showed acceptable PDI values < 0.5, which reflects a relatively homogeneous. Moreover, ZP values were > -30 mV, indicating high physical stability of the vesicles due to the electrostatic repulsive forces that prevent particle aggregation.

Furthermore, EE% increased significantly by increasing the amount of Span® 60 (p-value < 0.0001), or by increasing the amount of AP (p-value < 0.01), or by increasing both AP and Span® 60 amounts (p-value < 0.0001).

6.2.2. In vitro drug release at nasal conditions

The performance of FAV-ASP1 release at nasal conditions (pH 5.6) was evaluated in comparison to initial FAV, as shown in Figure 6. The result showed the FAV-ASP1 had a significantly higher cumulative release amount of FAV after 60 min in comparison to initial FAV (p-value < 0.001). This result could be attributed to the effect of AP, which reduces the surface tension, especially when integrated into a phospholipid monolayer. Therefore, the integration of AP with CH and Span® 60 could effect on the fluidity of the vesicle membrane resulting in higher release rate.

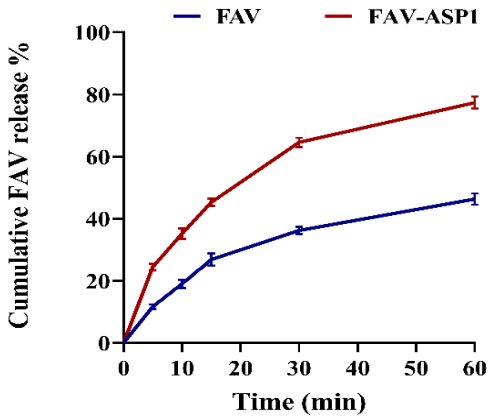

Figure 6. Cumulative *in vitro* release profile of FAV-ASP1 compared to pure FAV. Results are expressed as means ± SD (n = 3).

6.2.3. Ex vivo nasal diffusion study on human nasal mucosa

The result demonstrated that FAV-ASP1 had a significantly higher amount of FAV that permeated through the nasal mucosa compared to initial FAV within 60 min (1311.74 ± 41.70 µg/cm^2 and 128.17 ± 13.64 µg/cm^2, respectively), (p-value < 0.0001), as presented in Figure 7. This result demonstrates that using ASP as a drug carrier enhances drug permeation through the nasal mucosa, facilitating more efficient drug delivery via IN administration.

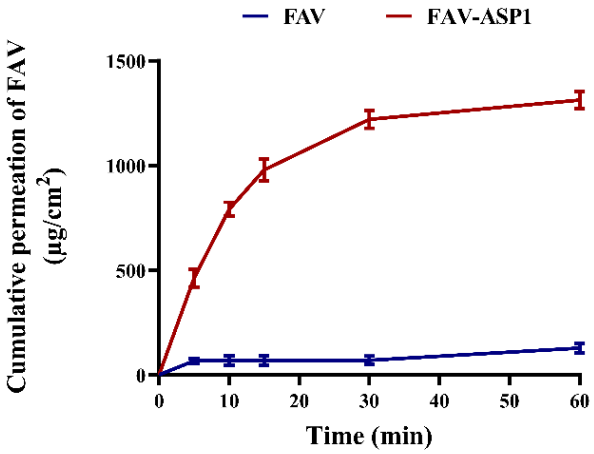

Figure 7. Ex vivo permeability study of FAV-ASP1 in comparison with initial FAV on human nasal mucosa. Results are expressed as means ± SD (n = 3).

6.2.4. In vivo study

6.2.4.1. Evaluation of pharmacokinetic (PK) parameters

FAV has low water solubility (8.7 mg/mL) and limited permeability to the CNS, which can be attributed to its low passive permeability caused by the presence of three hydrogen bond donors. The efficiency of formulations FAV-ASP1 to deliver FAV to the CNS after IN administration was tested using Sprague–Dawley rats.

The result demonstrated that FAV was successfully detected in the plasma (Figure 8), with a plasma concentration peak (Cmax) of 27.03 ± 6.88 and 26.24 ± 7.382 µg/mL at 7.5 ± 2.88 and 7.5 ± 2.88 min (T_{max}) after IN administration of FAV-ASP1 and initial FAV, respectively (as shown in Table 5).

Both FAV-ASP1 and initial FAV had the same T_{max}, which indicates that the similarity in the absorption rate. Moreover, FAV-ASP1 showed a higher half-life compared to the initial FAV (non-significant). FAV-ASP1 demonstrated a higher AUC0–t value, which reflects a higher actual body exposure to FAV after IN administration. The clearance values indicated that FAV-ASP1 had a slower elimination rate. The lower Vd value of FAV-ASP1 could mean a less distribution into tissues. However, FAV-ASP1 had a higher MRT value than the initial FAV, indicating a longer duration of FAV in the circulation system. As a result, FAV-ASP1 had a high relative bioavailability, indicating that ASP vesicles enhanced the bioavailability of FAV.

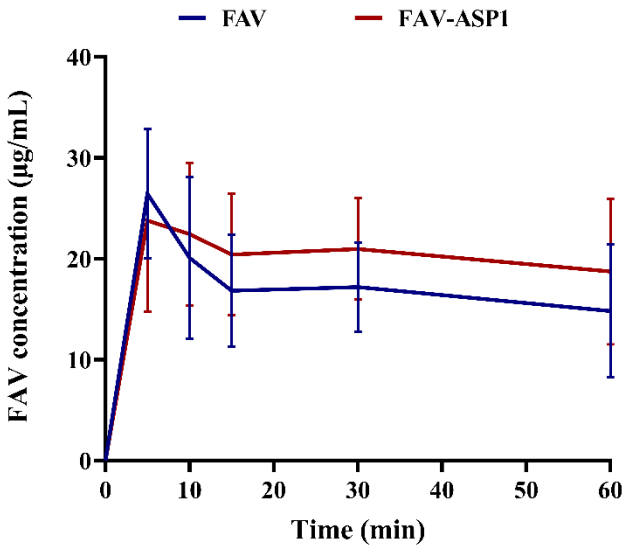

Figure 8. Plasma concentration–time profile after nasal administration of FAV-ASP1 and initial FAV in rats. Results are expressed as means ± SD (n = 4).

Table 5. Pharmacokinetic (PK) parameters of FAV-ASP1 and initial FAV after non-compartmental analysis. Results are expressed as means ± SD (n = 4).

PK parameters	**FAV**	**FAV-ASP8**
C_{max} (µg/mL)	26.24 ± 7.38	27.03 ± 6.88
T_{max} (min)	7.50 ± 2.88	7.50 ± 2.88
k_e (min^{-1})	0.007 ± 0.01	0.009 ± 0.005
$t_{1/2}$ (min)	127.54 ± 103.60	226.42 ± 337.06
AUC_{0-t} (µg × min/mL)	953.56 ± 282.31	1153.01 ± 364.87
$AUC_{0-\infty}$ (µg × min/mL)	4134.94 ± 4133.03	9305.40 ± 14438.56
C_L (mL/min)	0.88 ± 0.62	0.79 ± 0.56
V_d (mL)	104.57 ± 27.35	80.55 ± 19.01
MRT (min)	185.23 ± 153.68	329.96 ± 486.03
F (%)	-	124.53 ± 35.33

We evaluated the efficacy of ASP vesicles to deliver FAV to CNS by measuring the concentration of FAV in CSF samples after 1 h of the IN administration (Figure 9), where the olfactory nerve in the nasal cavity is considered a direct route to CNS, in addition to the direct link with the CSF in the subarachnoid space through the interstitial fluid surrounding the olfactory nerve bundle.

The result demonstrated that FAV was successfully reach the CSF, with a concentration of 8.29 ± 1.51 and 6.02 ± 1.04 µg/mL for FAV-ASP1 and initial FAV, respectively. The

significant higher concentration of FAV-ASP1 (*p-value < 0.05) could be attributed to an increase in the extent of drug absorption through the nasal mucosa (olfactory nerves) due to the physical parameter, the lipophilicity nature of the vesicles and the presence of a permeation enhancer (Span® 60), which improves the membrane penetration. Furthermore, AP can overcome biological barriers, enter the brain and resist hydrolysis, thereby preventing the degradation of FAV. According to the chemical structure of FAV, amide hydrolysis and oxidation are the potential major degradation pathways.

7. SUMMARY

Nose-to-brain delivery system could be a promising strategy for targeting the CNS, and overcome the bioavailability obstacles associated with oral administration such as poor solubility, first-pass hepatic metabolism, side effects and dose-dependent toxicity.

In this Ph.D. work, we selected BSA nanoparticles as a carrier for LAM, and ASP as a carrier for FAV. Both nanocarriers showed excellent nasal applicability results, including article size, surface charge, mucoadhesion properties, and drug encapsulation.

The optimal LAM-BSA formulation demonstrated a higher cumulative release amount at blood conditions compared to nasal conditions, which could be related to the pH-dependent solubility of LAM. Moreover, the in vitro permeability results showed an improved in the flux value of LAM through the porcine brain polar lipid extract. The ex vivo permeability result illustrated a higher diffusion of LAM from LAM-BSA formulation through the human nasal mucosa compared to the initial LAM. Finally, the cell line studies demonstrated that the use of BSA as a carrier of LAM reduced its cytotoxicity and improved its permeability through Caco-2 cells.

On the other hand, the optimal FAV-ASP formulation showed enhancement in the stability and solubility of FAV, with a higher release rate under both nasal and blood circulation conditions. The in vitro permeability results showed higher permeability and flux values of FAV through the porcine brain polar lipid extract in comparison to initial FAV. Moreover, FAV-ASP formulation had a higher diffusion of FAV through the human nasal mucosa compared to the initial FAV. The in vivo study indicated that there was no significant difference in plasma concentrations for FAV-ASP in comparison to initial FAV, while it had a significantly higher CSF concentrations. Additionally, IVIVC illustrated a good correlation between the in vitro and the in vivo PK data.

In summary, LAM-BSA and FAV-ASP could be a promising drug delivery systems for targeting the CNS, improve the bioavailability and reduce the adverse effects of the drugs.

PUBLICATIONS RELATED TO THE THESIS:

- **Salamah, M.;** Volk, B.; Lekli, I.; Bak, I.; Gyöngyösi, A.; Kozma, G.; Kónya, Z.; Szalenkó-Tőkés, Á.; Kiricsi, Á.; Rovó, L.; et al. Preparation, and Ex Vivo and in Vivo Characterization of Favipiravir-Loaded Aspasomes and Niosomes for Nose-to-Brain Administration. Int J Nanomedicine 2025, 20, 6489–6514, doi:10.2147/IJN.S518486.
  (D1, IF: 6.5).
- **Salamah, M.;** Sipos, B.; Schelz, Z.; Zupkó, I.; Kiricsi, Á.; Szalenkó-Tőkés, Á.; Rovó, L.; Katona, G.; Balogh, G.T.; Csóka, I. Development, in Vitro and Ex Vivo Characterization of Lamotrigine-Loaded Bovine Serum Albumin Nanoparticles Using QbD Approach. Drug Deliv 2025, 32, doi:10.1080/10717544.2025.2460693.
  (D1, IF: 6.5).

PUBLICATIONS NOT RELATED TO THE THESIS:

- **Salamah, M.;** Sipos, B.; Katona, G.; Volk, B.; Balogh, G.T.; Csóka, I. Development and Validation of a Novel Isocratic RP-HPLC Method Using AQbD Approach for the Quantification of Favipiravir. European Journal of Pharmaceutical Sciences 2025, 214, 107276, doi:10.1016/J.EJPS.2025.107276.
  (Q1, IF: 4.7).
- **Salamah, M.;** Budai-Szűcs M.; Sipos, B.; Volk, B.; Katona, G.; Tibor Balogh, G.; Csóka, I. Development and Characterization of In Situ Gelling Nasal Cilostazol Spanlastics. Gels 2025, Vol. 11, Page 82 2025, 11, 82, doi:10.3390/GELS11020082.
  (Q1, IF: 5.3).
- Balogh-Weiser, D.; Molnár, A.; Tóth, G. D.; Koplányi, G.; Szemes, J.; Decsi, B.; Katona, G.; **Salamah, M.;** Ender, F.; Kovács, A.; Berkó, S.; Budai-Szűcs, M.; Balogh, G. T. Combined Nanofibrous Face Mask: Co-Formulation of Lipases and Antibiotic Agent by Electrospinning Technique. Pharmaceutics 2023, 15 (4), 1174. https://doi.org/10.3390/pharmaceutics15041174.
  (Q1, IF: 4.9).

PRESENTATIONS RELATED TO THE SUBJECT OF THE THESIS

A. Oral presentations

1) **Salamah, M.;** Balogh, G.T.; Katona, G. (2022). Improving the bioavailability of Favipiravir by using human serum albumin nanoparticles. IV. Symposium of Young Researchers on Pharmaceutical Technology, Biotechnology and Regulatory Science, Szeged, Hungary.
2) **Salamah, M.;** Balogh, G.T.; Katona, G. (2023). Formulation and Optimization of Lamotrigine-Loaded Bovine Serum Albumin Nanoparticles by Using Full Factorial Design. V. Symposium of

Young Researchers on Pharmaceutical Technology, Biotechnology and Regulatory Science, Szeged, Hungary.

3) **Salamah, M.;** Balogh, G.T.; Katona, G. (2023). Preparation, *in vitro* and *ex vivo* evaluation of favipiravir loaded niosomes for nose-to-brain administration. Medicinal Chemistry and Pharmaceutical Technology Symposium '23, Herceghalom, Hungary.
4) **Salamah, M.;** G.; Katona, G. (2023). Quality by Design Approach for Optimization of Lamotrigine-Loaded Bovine Serum Albumin Nanoparticles for Intranasal Administration. XV. Ottó Clauder Memorial Competition, Budapest, Hungary.
5) **Salamah, M.;** Balogh, G.T.; Katona, G. (2024). Formulation and optimization of rifampicin-loaded niosomes for ocular delivery system. VI. Symposium of Young Researchers on Pharmaceutical Technology, Biotechnology and Regulatory Science, Szeged, Hungary.
6) Katona, G.; **Salamah, M.;** Sipos, B.; Schelz, Z.; Zupkó, I.; Balogh, G.T.; Csóka, I. (2024). Investigation of the Effect of Different Cross-Linking Agents on the Colloidal Properties of Albumin Nanoparticles. Congressus Pharmaceuticus Hungaricus XVII. and EUFEPS Annual Meeting, Debrecen, Hungary.
7) **Salamah, M.;** Balogh, G.T.; Katona, G. (2024). Rifampicin-loaded niosomes: optimization, *in vitro* and *ex vivo* characterization. XXVII. Spring Wind Conference, Budapest, Hungary.
8) **Salamah, M.;** Volk, B.; Csóka, I.; Balogh, G.T.; Katona, G. (2024). Novel mucoadhesion chitosomes for nose-to-brain delivery of favipiravir. 7th Young Technologists' Forum, Budapest, Hungary.
9) **Salamah, M.;** Budai-Szűcs M.; Sipos, B.; Volk, B.; Katona, G.; Tibor Balogh, G.; Csóka, I. (2025). Cilostazol spanlastic vesicles-loaded in situ gel for nose-to-brain delivery system. VII. Symposium of Young Researchers on Pharmaceutical Technology, Biotechnology and Regulatory Science, Szeged, Hungary.
10) **Salamah, M.;** Balogh, G.T.; Katona, G. (2025). Rifampicin-loaded lipidic liquid-crystalline phases (cubosomes) for nose-to-brain delivery system for CNS tuberculosis. 8th Young Technologists' Forum, Budapest, Hungary.

B. Poster presentations

1) **Salamah, M.;** Balogh, G.T.; Katona, G. (2023). Preparation, *In Vitro* and *Ex Vivo* Characterization of Lamotrigine-Loaded Bovine Serum Albumin Nanoparticles Using QbD Approach. European Federation for Pharmaceutical Sciences (EUFEPS) Annual meeting, Lisbon, Portugal.
2) **Salamah, M.;** Balogh, G.T.; Katona, G. (2025). Doxorubicin-loaded cubosomes functionalized with hyaluronic acid for intranasal administration. 1st International Health Science Conference Szeged, Szeged, Hungary.
3) **Salamah, M.;** Volk, B.; Lekli, I.; Bak, I.; Gyöngyösi, A.; Csóka, I.; Balogh, G.T.; Katona, G. (2025). Evaluation of *in vivo* nose-to-brain delivery of favipiravir-loaded aspasomes. 15th Central European Symposium on Pharmaceutical Technology, Bled, Slovenia**.**

ACKNOWLEDGEMENTS

Family first, always and forever. This PhD dissertation is a reflection of the unwavering love, support and encouragement of my family through this journey, which has been fraught with both professional and personal challenges. I owe an immense debt of gratitude to my parents for their endless love and sacrifices. For my brothers, my strength, I am deeply grateful for your belief in me and for lifting me during all challenges, especially Dr. Zain. For my niblings, my little angels, I love you all. For my niece, Meryam, you will always be my little daughter and my sunshine.

A heartfelt thank you to **Dr. Gábor Katona**, my supervisor, for your kindness, exceptional guidance, constant support, trust and motivation. I feel privileged to have your guidance and mentorship on this journey.

My sincere appreciation to my supervisor, **Prof. Dr. György Tibor Balogh**, for his constructive feedback and support that enhanced my PhD work and my academic journey.

Additionally, I would like to acknowledge **Prof. Dr. Ildikó Csóka**, the head of the Institute of Pharmaceutical Technology and Regulatory Affairs, and **Prof. Dr. Rita Ambrus** for providing the resources and facilities necessary to conduct my research.

I am equally thankful for **Prof. Dr. István Zupkó**, the head of the Institute of Pharmacodynamics and Biopharmacy, for the collaboration and contribution which made this research possible.

I would like to express my deep gratitude to everyone who contributed to the completion of this thesis: **Dr. Bence Sipos** and **Dr. Mária Budai-Szűcs** from Institute of Pharmaceutical Technology and Regulatory Affairs; **Dr. Zsuzsanna Schelz** from the Institute of Pharmacodynamics and Biopharmacy, University of Szeged; **Dr. István Lekli, Dr. István Bak, Alexandra Gyöngyösi** from the Department of Pharmacology, University of Debrecen; **Prof. Dr. Gábor Kozma and Prof. Dr. Zoltán Kónya** from the Department of Applied & Environmental Chemistry, University of Szeged; **Prof. Dr. László Rovó, Dr. Ágnes Szalenkó-Tőkés** and **Dr. Ágnes Kiricsi** from the Department of Oto-Rhino-Laryngology and Head-Neck Surgery, University of Szeged; **Dr. Diana Balogh-Weiser** from the Department of Physical Chemistry and Materials Science, Budapest University of Technology and Economics; and **Dr. Balázs Volk** from Egis Pharmaceuticals Plc.

I would like to extend my sincere thanks to my lab colleagues and the administrative and technical staff in the institute for their support and making this journey easier for me.

Finally, I must also express my deepest appreciation for my second family, for their unconditional love, encouragement and continuous support. To my supervisor in Syria, **Dr. Yousef Al-Ahmad** and his wife, **Ms. Nesreen Alkhadour**, for your friendship, for being always there for me in my bad and good days and accepting me as a family member. To **Nawar Alkhadour,** I am grateful for

having you here with me in this journey. To **Prof. Dr. Hala Deeb,** a heartfelt gratitude for the chance that led me to meet you, I cherish your presence in my life. To **Hanan Makhlof**, a friend in the sense of a sister, thank you for always being there for me. To **Shady Ashy**, my young brother, thank you for making me feel like a home away from home. To my friend for all times and memories, **Dr. Walaa Salamah**, thank you for standing by me. For who believed in me and supported me to pursue my academic journey, **Dr. Haifaa Al-Ali**, may your soul rest in peace.

To **Dr. Mahwash Mukhtar** and **Dr. Zsófia Németh**, for their friendship, motivation and willingness to listen, which have made this journey easier.

To my sustenance in life, the shoulder to cry on, my dear friends: **Dr. Suha Alnaeb, Lina Soliman, Lomass Soliman, Fatima Rajab, Hiba Alsoliman, Ola Salamah, Hanan Mohammad**, I am truly grateful for the strength you have given me.

To the gift of my life, the peace amidst chaos, and the light during my darkest days,

thank you.

FINANCIAL SUPPORT

This PhD work was generously supported by the Stipendium Hungaricum Program, and by Project no. TKP2021-EGA-32 implemented with support provided by the Ministry of Culture and Innovation of Hungary from the National Research, Development and Innovation Fund, financed under the TKP2021-EGA funding scheme.